The following article appeared in *Journal of Ceramic Science and Technology 7(3): 289-294, 2017*; and may be found at: http://dx.doi.org/10.4416/JCST2016-00020

Journal of
Ceramic Science
and Technology

J. Ceram. Sci. Tech., 07 [03] 289-294 (2016)
DOI: 10.4416/JCST2016-00020
available online at: http://www.ceramic-science.com

Facile Synthesis and Characterization of $Mn_xZn_{1-x}Fe_2O_4$/Activated Carbon Composites for Biomedical Applications

J.C. Ríos-Hurtado[1], A.C. Martínez-Valdés[1], J.R. Rangel-Méndez[2], J.C. Ballesteros-Pacheco[1], E.M. Múzquiz-Ramos*[1]

[1]Facultad de Ciencias Químicas, Universidad Autónoma de Coahuila,
Blvd. V. Carranza y José Cárdenas Valdés, C.P. 25280, Saltillo, México.
[2]División de Ciencias Ambientales, Instituto Potosino de Investigación Científica y Tecnológica A.C.,
Camino a la Presa de San José 2055, Col. Lomas 4ª Sección, C.P. 78216, San Luis Potosí. México.

received Febuary 24, 2016; received in revised form April 20, 2016; accepted May 15, 2016

Abstract

The synthesis of $Mn_xZn_{1-x}Fe_2O_4$ ferrites (x = 0.4, 0.5 and 0.6) by means of the co-precipitation method is reported. Furthermore, a composite of $Mn_{0.4}Zn_{0.6}Fe_2O_4$/activated carbon was prepared with the mechanosynthesis method. The magnetic, structural, morphological and chemical properties were analyzed by means of VSM, XRD, SEM, FTIR and Boehm's titration. The heating capacity was evaluated under a magnetic field using solid-state induction heating equipment, in addition a hemolysis test was performed using human red blood cells. With regard to the synthesis of manganese-zinc ferrite, the results indicated that $Mn_{0.4}Zn_{0.6}Fe_2O_4$ ferrite showed higher saturation magnetization (64.48 emu/g) than the other ferrite obtained, with superparamagnetic behavior. The $Mn_{0.4}Zn_{0.6}Fe_2O_4$/activated carbon composite was able to heat in concentrations of 10 mg/ml under a magnetic field (10.2 kAm^{-1} and frequency 200 kHz), increasing the temperature up to 42.5 °C. The hemolysis test indicated that the presence of activated carbon reduces the hemolytic behavior of the ferrite. Thanks to its heating capacity and non-hemolytic activity, the $Mn_{0.4}Zn_{0.6}Fe_2O_4$/activated carbon composite is a potential candidate for use in biomedical applications.

Keywords: Mn-Zn ferrite, superparamagnetic, activated carbon, composite, hemolysis.

I. Introduction

The development of magnetic nanoparticles has been studied extensively with regard to their utilization in biomedical applications because of their suitable magnetic properties and ability to function at the cellular and molecular level of biological interactions [1]. All synthetic magnetic nanomaterials present advantages depending on their structural, morphological, chemical composition, and magnetic properties [2]. Magnetite (Fe_3O_4) and maghemite (γ-Fe_2O_3) are the ferrites more commonly used in biomedical applications, however, recent studies have reported the synthesis of compounds related to magnetite (inverse spinel), with the substitution of Fe^{2+} ions by metallic ions such as cobalt, nickel, manganese and zinc [3].

Manganese-zinc ferrites represent an important class of soft-magnetic materials. They are preferred over other ferrites because of their high saturation magnetization [4], high initial permeability, low losses, and relatively high Curie temperature, having wide applications such as soft-magnetic powders, hyperthermia, magnetic fluids, heat transfer systems [5].

These materials are obtained with several methods, however, the co-precipitation technique is a simple, low-cost and viable method for the synthesis of ferrites. Zhang *et al.* [6] synthesized manganese-zinc ferrites with cobalt doped by means of co-precipitation. Gopalan *et al.* [7] obtained $Mn_{1-x}Zn_xFe_2O_4$ by means of co-precipitation using metallic chlorides. Elahi *et al.*[8] obtained manganese-zinc ferrites with a particle size around 27 nm, they also utilized co-precipitation. Shijie *et al.* [9] synthesized manganese-zinc ferrites by means of co-precipitation and improved the heating treatment. It is important to note that the synthesis of Mn-Zn ferrites with the co-precipitation method implicates the use of thermal treatment at temperatures above 1150 °C, this being a disadvantage on account of the energy consumption. In this work, we present a rapid and direct route for the synthesis of $Mn_{1-x}Zn_xFe_2O_4$ with the co-precipitation method at pH 10 ± 0.1. This synthesis route exhibits advantages over other methods for the preparation of Mn-Zn ferrites in that the process does not involve high-temperature conditions for the production of nanometric particles.

Furthermore, different studies are focused on the use of these ferrites with coatings such as chitosan [10] and activated carbon [11, 12] for biomedical applications. Activated carbon offers an attractive and inexpensive option for coating owing to its large surface area and porous structure [13]. These characteristics have prompted many authors to use activated carbon and ferrites for drug delivery [14–16] owing to the adsorptive properties. Since it has been demonstrated that diverse types of activated carbon are biocompati-

* Corresponding author: emuzquiz@uadec.edu.mx

ble [17,18], it is possible to coat ferrites with activated carbon for biomedical applications.

The *in vitro* cytotoxicity assays are the primary biocompatibility screening tests for a wide variety of materials used in medical devices. Current experience indicates that a material judged to be non-toxic *in vitro* will also be non-toxic in *in vivo* assays [19].

Hyperthermia is one of the clinical tools used as coadjuvant therapy for cancer treatment. A clear synergistic effect has been demonstrated when it is combined with radiotherapy, and enhancing effects have been observed with numerous cytotoxic drugs. The viability of the cancerous cells is reduced and their sensitivity to chemotherapy and radiation is increased by raising the temperature of the target tissue to 42 – 46 °C [20]. Hyperthermia can be induced using magnetic nanoparticles, in a treatment known as magnetic hyperthermia. The nanoparticles can be introduced into the human body in the region surrounding the cancer tumor and then heated with the help of an external magnetic field. One of the crucial steps for magnetic hyperthermia application is the temperature control of the magnetic nanoparticles *in vivo* to avoid any damage to the surrounding normal tissue as a result of overheating. One possible approach to control the temperature is to design the materials in such a way that it exhibits temperature-sensitive magnetic properties [21].

The aim of this work was to obtain Mn-Zn ferrites by means of a rapid and easy co-precipitation method without thermal treatment; the Mn-Zn ferrites were to exhibit high saturation magnetization in order to improve the heating properties. Additionally, with the aim of increasing the activity of synthesized $Mn_xZn_{1-x}Fe_2O_4$ materials, $Mn_{0.4}Zn_{0.6}Fe_2O_4$ was mixed with activated carbon to obtain a new magnetic composite that can be used in biomedical applications such as the hyperthermia technique for cancer treatment.

II. Experimental

(1) Mn-Zn ferrites synthesis with modification of the manganese and zinc proportions

In accordance with the process reported in the literature by Zhang *et al.* [6], the manganese-zinc ferrite was synthesized. In a 500-mL ball flask, ammonium hydroxide and ammonium bicarbonate solution were placed in a ratio of 1.2 mL of NH_4HCO_3 for each mL of NH_4OH (pH 10 ± 0.1) at 50 °C under constant stirring. Simultaneously, a solution containing metal ions Fe^{+2} ($FeSO_4{\cdot}7H_2O$), Zn^{+2} ($ZnSO_4{\cdot}7H_2O$) and Mn^{+2} ($MnSO_4{\cdot}H_2O$) was prepared. The stoichiometric ratios were varied in order to obtain the ferrites summarized in Table 1. The solution containing ions was added drop by drop to the flask and constantly stirred for one hour. To complete the process, the precipitate obtained was washed with deionized water to remove the residual sulfates and allowed to dry at room temperature for three days. Finally, the precipitate was washed with ethanol and allowed to dry for 24 h at room temperature.

Table 1: Synthesized ferrites.

Sample	Mn (mol)	Zn (mol)	Fe (mol)
$Mn_{0.4}Zn_{0.6}Fe_2O_4$	0.4	0.6	2
$Mn_{0.5}Zn_{0.5}Fe_2O_4$	0.5	0.5	2
$Mn_{0.6}Zn_{0.4}Fe_2O_4$	0.6	0.4	2

(2) $Mn_{0.4}Zn_{0.6}Fe_2O_4$ /GAC composite mechanosynthesis

The obtained Mn-Zn ferrite with the highest saturation magnetization ($Mn_{0.4}Zn_{0.6}Fe_2O_4$) and the granular activated carbon (GAC) were placed into an agate container of a FRITSCH planetary mill (Pulverisette 6) for mechanosynthesis treatment. A mass proportion of 60 % $Mn_{0.4}Zn_{0.6}Fe_2O_4$ and 40 % GAC were used. The procedure was conducted at 400 rpm for 3 h. Finally, the composite ($Mn_{0.4}Zn_{0.6}Fe_2O_4$/GAC) was washed with deionized water and allowed to dry at room temperature.

(3) Characterization

The obtained Mn-Zn ferrites nanoparticles and the composite $Mn_{0.4}Zn_{0.6}Fe_2O_4$/GAC were analyzed with x-ray diffraction (XRD) (Siemens Mod. D-5000). Magnetic properties of the samples were measured with a SQUID Quantum Design magnetometer (VSM) in applied fields from - 20 to 20 kOe at room temperature. The GAC and composite surface were studied by means of field emission scanning electron microscopy (SEM) (JEOL JSM-7401F). Moreover, in order to determine the active sites in the GAC and composite surface, FTIR analysis and a Boehm's titration study [22] were conducted.

(4) Tests for biomedical applications

The synthesized materials ($Mn_{0.4}Zn_{0.6}Fe_2O_4$ and $Mn_{0.4}Zn_{0.6}Fe_2O_4$/GAC) were tested in order to determine the effectiveness of heat generation under a magnetic field. Tests for heating capacity were conducted as reported in our previous work [23], using a magnetic field of 10.2 kA/m and a frequency of 200 kHz.

Moreover, in order to determine the biocompatibility of $Mn_{0.4}Zn_{0.6}Fe_2O_4$/GAC with erythrocytes, hemolysis tests were conducted, using human red blood cells from healthy non-smoking donors, following the proper guidelines for studies using human specimens. The procedure was conducted as reported by Múzquiz-Ramos *et al.* in 2014 [19]. Erythrocytes suspensions were incubated with the $Mn_{0.4}Zn_{0.6}Fe_2O_4$ ferrite and the composite ($Mn_{0.4}Zn_{0.6}Fe_2O_4$/GAC). Three concentrations of particles were tested: 0.5, 2.0 and 3.0 g/L.

III. Results and Discussions

(1) Ferrite properties

Since it has been demonstrated in the hyperthermia technique that the saturation magnetization (Ms) is directly proportional to heating capacity for hyperthermia [21], the magnetic properties of the synthesized ferrites were determinate. As it is well known, for all cases of ferromagnetic

spinels with a cubic system, the magnetic order is mainly due to a super exchange interaction mechanism occurring between the metal ions in the A and B sublattices. The substitution of nonmagnetic ion such as Zn, which has a preferential A site occupancy, provokes the reduction of the exchange interaction between A and B sites. Hence, by varying the degree of zinc substitution, it is possible to vary the magnetic properties of the synthesized ferrites.

Fig. 1 shows the dependence between magnetic field and magnetization (M-H curve) at room temperature for the synthesized Mn-Zn ferrites for different manganese and zinc substitutions, where an increase in Zn substitution reaches a maximum value of 64.48 emu/g for x = 0.4 (Fig. 1a) and the hysteresis loops show low coercivity and high magnetic permeability.

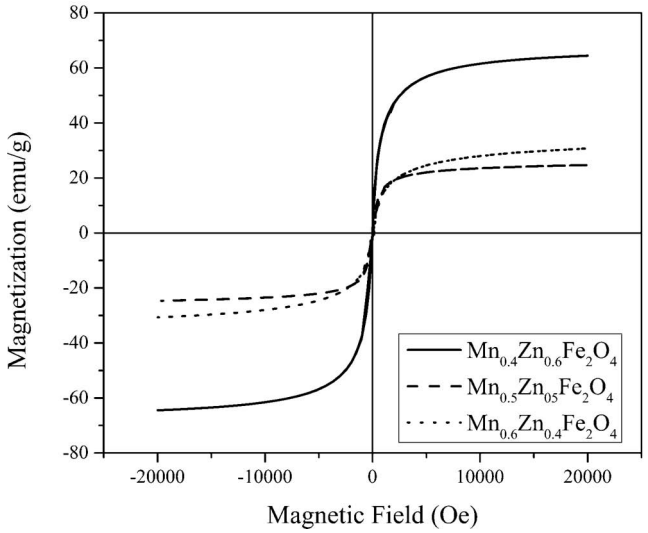

Fig. 1: Hysteresis loops for Mn-Zn synthesized ferrites.

The saturation magnetization (M_s), remanence magnetization (M_r) and coercivity (H_c) values are summarized in Table 2. As observed, the saturation magnetization decreased and the coercivity values increased when values of manganese were higher. Caltun *et al.* suggested that variation of the saturation magnetization depends on the cation distribution in a spinel lattice [24]. Moreover, the magnetomechanical hysteresis, which depends on the magnetocrystalline anisotropy, is therefore expected to decrease, as the coercivity does [25].

Fig. 2 shows the XRD patterns of synthesized Mn-Zn ferrites. The indexed diffraction peaks for $Mn_{0.4}Zn_{0.6}Fe_2O_4$ ferrite were consistent with the standard JCPDS data of inverse spinel ferrite (Card no. 19–629), revealing a cubic spinel crystal structure. No other diffraction signals were detected. The crystallite size calculated with Scherrer's equation was 9.43 nm, which can be a result of the synthesis method. It is important to mention that this ferrite was synthesized without thermal treatment.

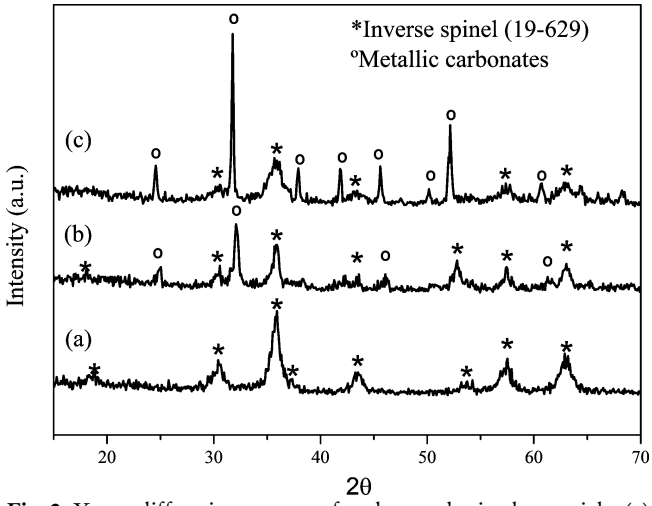

Fig. 2: X-ray diffraction patterns for the synthesized materials. (a) $Mn_{0.4}Zn_{0.6}$ Fe_2O_4. (b) $Mn_{0.5}Zn_{0.5}$ Fe_2O_4. (c) $Mn_{0.6}Zn_{0.4}$ Fe_2O_4.

When manganese substitution increases, new signals appear, revealing the presence of metallic carbonates, as $FeCO_3$ and $MnCO_3$ (Figs. 2b and 2c). This implies that a higher manganese concentration produces a mix of this species and the inverse spinel ferrites; this is the reason why Ms decreases. Finally, on the basis of its high magnetization saturation and low coercivity it is possible to conclude that the best ferrite was $Mn_{0.4}Zn_{0.6}Fe_2O_4$, which may be useful for magnetic hyperthermia treatment.

(2) Composite characteristics

The magnetic hysteresis loop (Fig. 3) of the composite is presented. A decrease in Ms (37.76 emu/g) is observed owing to the presence of the GAC. In Table 3 a comparison of magnetic properties of the $Mn_{0.4}Zn_{0.6}Fe_2O_4$ ferrite and composite is presented. The registered values indicate that a decrease in all magnetic properties occurs, which is due to the incorporation of activated carbon, since it is a diamagnetic material. It is relevant that this type of material has no coercivity nor remanence, which means that when the external magnetic field is switched off, the internal magnetic dipoles randomize again and no extra energy is required to demagnetize the material and hence the initial zero net magnetic moment is spontaneously recovered [26]. This characteristic is important for the use of the materials in biomedical applications.

Table 2: Magnetic properties of synthesized Mn-Zn ferrites.

Ferrite	Magnetization M_s (emu/g)	Remanence M_r (emu/g)	Coercivity H_c (Oe)
$Mn_{0.4}Zn_{0.6}$ Fe_2O_4	64.48	0.88	9.61
$Mn_{0.5}Zn_{0.5}$ Fe_2O_4	24.69	0.48	19.86
$Mn_{0.6}Zn_{0.4}$ Fe_2O_4	30.71	0.12	43.09

Table 3: Comparison of magnetic properties of $Mn_{0.4}Zn_{0.6}Fe_2O_4$ ferrite and $Mn_{0.4}Zn_{0.6}Fe_2O_4$ /GAC composite.

Ferrite	Magnetization M_s (emu/g)	Remanence M_r (emu/g)	Coercivity H_c (Oe)
$Mn_{0.4}Zn_{0.6}Fe_2O_4$	64.48	0.88	9.61
Composite	37.76	0.28	0.01

Fig. 4 shows an SEM micrograph of a representative sample of the composite, which confirms uniform, spherical-shaped and agglomerated particles. The surface morphology shows compact and regular arrangement of nanoparticles in the GAC surface. It can be concluded that the particles and the agglomerates were anchored to the GAC surface. The agglomerates are structures consisting of many smaller ferrite units. Spherical particles predominate, with a size between 8 – 15 nm. These values were comparable with the crystallite size obtained with Scherrer's equation (9.43 nm).

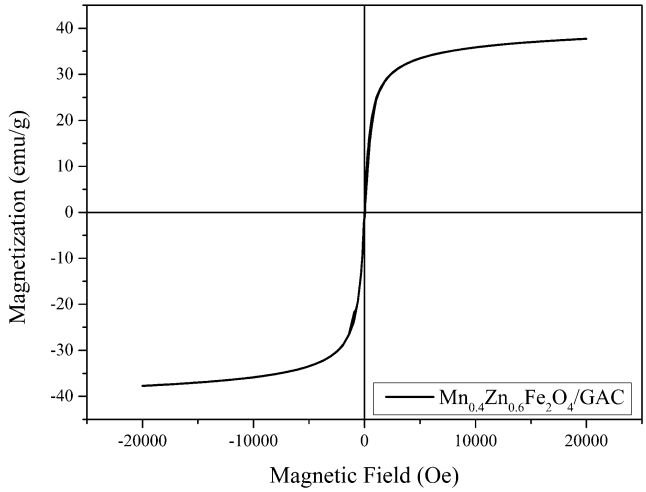

Fig. 3: Magnetic hysteresis loop of $Mn_{0.4}Zn_{0.6}Fe_2O_4$/GAC composite.

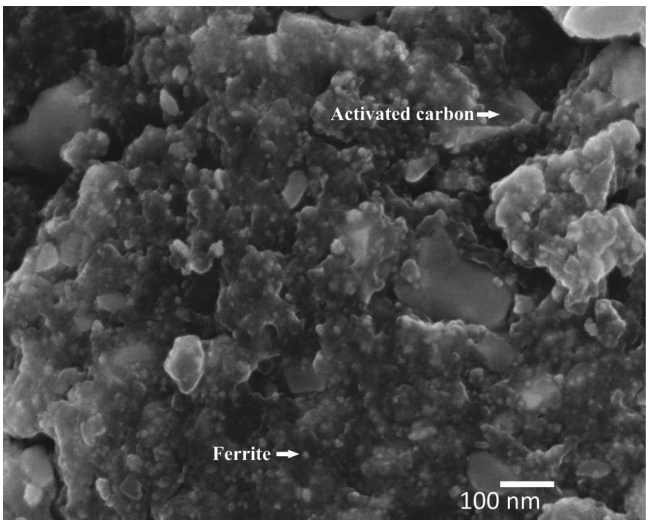

Fig. 4: SEM image for $Mn_{0.4}Zn_{0.6}Fe_2O_4$/GAC composite surface.

In order to determine the interaction between the GAC surface and the ferrite, shown in Fig. 5 are the FTIR spectra of the GAC and the composite ($Mn_{0.4}Zn_{0.6}Fe_2O_4$/GAC) at room temperature in the frequency range of 4000 – 600 cm^{-1}. For the GAC sample, a series of absorption bands corresponding to symmetric vibration of COO group between 1750 – 1600 cm^{-1} are observed and one more at around 3500 cm^{-1} corresponding to the symmetric vibration of the O-H group.

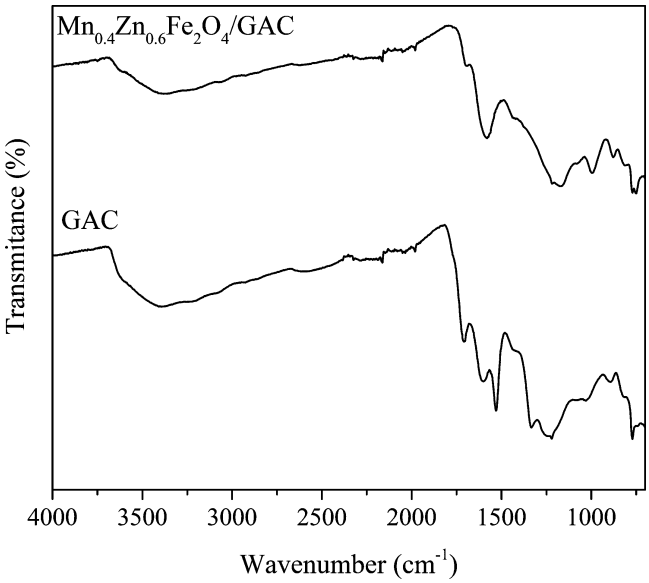

Fig. 5: IR-FT spectra for GAC and for $Mn_{0.4}Zn_{0.6}Fe_2O_4$/GAC composite.

On the other hand, in the composite the absorptions bands between 1750 and 1600 cm^{-1} show lower intensity and seems to be united in a stretch band near 1633 cm^{-1}, indicating a possible anchorage of the $Mn_{0.4}Zn_{0.6}Fe_2O_4$ ferrite in oxygenated groups of the GAC surface. Furthermore, a band near 600 cm^{-1} appears for the composite, which is ascribed to the stretching vibration of octahedral and tetrahedral metal-oxygen bonds. These results allow us to propose that the formation of $Mn_{0.4}Zn_{0.6}Fe_2O_4$/GAC composite has occurred.

Boehm's titration was conducted to determine active sites in the GAC surface and in the composite surface, in order to confirm the anchorage of ferrite $Mn_{0.4}Zn_{0.6}Fe_2O_4$. In Table 4 the values of active sites are summarized. All active sites decrease for the composite. These results indicate that the acid-active sites of the GAC surface bonded the $Mn_{0.4}Zn_{0.6}Fe_2O_4$ ferrite, the results compared with those observed in infrared spectroscopy.

Table 4: Surface-active sites in GAC and $Mn_{0.4}Zn_{0.6}Fe_2O_4$/GAC composite.

Sample	Carboxylic (meq/g)	Lactonic (meq/g)	Phenolic (meq/g)	Total (meq/g)
GAC	2.645	2.490	3.645	8.784
Composite	0.995	1.497	1.992	4.485

(3) Composite biomedical applications

In order to determine if the obtained magnetic nanoparticles and composite can be used for hyperthermia treatment, it is necessary to evaluate the heating capacity of the materials on application of a magnetic field. Fig. 6 shows the heating curves obtained under an applied magnetic field of 10.2 kAm^{-1} and frequency of 200 kHz, conditions within the range of that allowed for human body. The measured concentrations were 6.5 mg/mL for $Mn_{0.4}Zn_{0.6}Fe_2O_4$ ferrite and 10 mg/mL for $Mn_{0.4}Zn_{0.6}Fe_2O_4$/GAC composite. The concentration of composite is increased since the GAC does not have any magnetic properties. The behavior of the samples differs but the temperature reached after 15 min is the same (42.5 °C). This temperature is adequate for magnetic hyperthermia for cancer treatment [20]. The amount of magnetic material required to produce the required temperatures depends to a large extent on the method of administration. A reasonable assumption is that 5 – 10 mg magnetic material concentrated in each cm^3 of tumor tissue is appropriate for magnetic hyperthermia in human patients. The concentration that we have tested is adequate for a 1-cm^3 tumor [27].

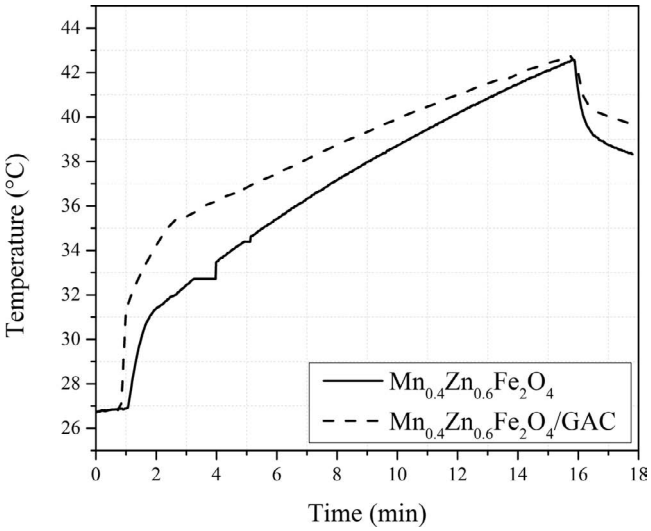

Fig. 6: Heating curves of $Mn_{0.4}Zn_{0.6}$ Fe_2O_4 ferrite (6.5 mg/mL) and for $Mn_{0.4}Zn_{0.6}Fe_2O_4$/GAC composite (9 mg/mL)..

Fig. 7 shows the hemolysis percentages caused by $Mn_{0.4}Zn_{0.6}Fe_2O_4$ ferrite and $Mn_{0.4}Zn_{0.6}Fe_2O_4$/GAC composite. It is observed that the hemolysis percentage increases at higher concentrations. A non-hemolytic material is described as a material that does not cause more than 5 % hemolysis [28], $Mn_{0.4}Zn_{0.6}Fe_2O_4$ ferrite can be a hemolytic material in higher concentrations (up to 2.0 g/L), however, when the ferrite is diluted with GAC in the composite, the hemolysis percentage decreases, giving the $Mn_{0.4}Zn_{0.6}Fe_2O_4$/GAC composite an excellent characteristic for any biomedical applications, since the hemolysis percentage is no higher than 5 % at concentrations around 3.0 g/L.

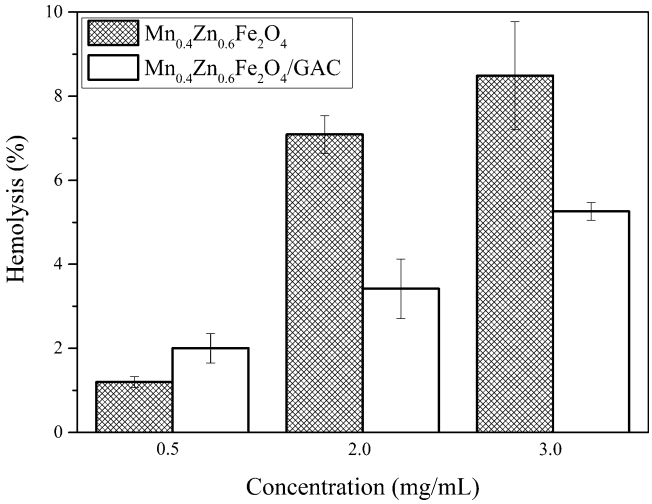

Fig. 7: Hemolysis for $Mn_{0.4}Zn_{0.6}Fe_2O_4$ ferrite and $Mn_{0.4}Zn_{0.6}Fe_2O_4$/GAC composite.

IV. Conclusions

$Mn_{0.4}Zn_{0.6}Fe_2O_4$ was obtained with a simple co-precipitation technique without heating treatment. This material and GAC were treated by mechanosynthesis to obtain a composite ($Mn_{0.4}Zn_{0.6}Fe_2O_4$/GAC,) with appropriate magnetic properties. SEM images, FTIR spectra and Boehm's titration showed that the ferrites seem to be anchored to oxygenated functional groups in the GAC surface. The composite might be a potential material for cancer treatment based on magnetic hyperthermia therapy, since non-hemolytic behavior was observed and reached a temperature of 42.5 °C under a low magnetic field.

Acknowledgments

J.C. Ríos Hurtado thanks CONACyT-Mexico for the financial support (scholarship 423185).

References

1 Karimi, Z., Karimi, L., Shokrollahi, H.: Nano-magnetic particles used in biomedicine: Core and coating materials. *Mater. Sci. Eng. C*, **33**, 2465 – 2475, (2013).

2 Dumitrescu, A.M., Slatineanu, T., Poiata, A., Iordan, A.R.: Colloids and surfaces A: Physicochemical and engineering aspects advanced composite materials based on hydrogels and ferrites for potential biomedical applications. *Colloids Surface A*, **455**, 185 – 194, (2014).

3 Mahmoudi, M., Sant, S., Wang, B., Laurent, S., Sen, T.: Superparamagnetic iron oxide nanoparticles (SPIONs): development, surface modification and applications in chemotherapy, *Adv. Drug Deliv. Rev.*, **63**, 24 – 46, (2011).

4 Harris, V.G. *et al.*: Recent advances in processing and applications of microwave ferrites. *J. Magn. Magn. Mater.*, **321**, 2035 – 2047, (2009).

5 Iftikhar, A. *et al.*: Synthesis of super paramagnetic particles of $Mn_{1-x}Mg_xFe_2O_4$ ferrites for hyperthermia applications, *J. Alloys Compd.*, **601**, 116 – 119, (2014).

6 Zhang, C.F., Zhong, X.C., Yu, H.Y., Liu, Z.W., Zeng, D.C.Ã.: Effects of cobalt doping on the microstructure and magnetic properties of Mn – Zn ferrites prepared by the co-precipitation method, *Phys. B*, **404**, 2327 – 2331, (2009).

7 Veena Gopalan, E. *et al.*: Impact of zinc substitution on the structural and magnetic properties of chemically derived nanosized manganese zinc mixed ferrites, *J. Magn. Magn. Mater.*, **321**, 1092 – 1099, (2009).

8 Elahi, I., Zahira, R., Mehmood, K., Jamil, A., Amin, N.: Co-precipitation synthesis, physical and magnetic properties of manganese ferrite powder, *African J. Pure Appl. Chem.*, **6**, 1 – 5, (2012).

9 Chen, S., Xia, J., Dai, J.: Effects of heating processing on microstructure and magnetic properties of mn-zn ferrites prepared via chemical co-precipitation, *J. Wuhan Univ. Technol. Sci. Ed.*, **30**, 684 – 688, (2015).

10 Zahraei, M. *et al.*: Synthesis and characterization of chitosan coated manganese zinc ferrite nanoparticles as MRI contrast agents, *J. Nanostructures*, **5**, 77 – 86, (2015).

11 Yang, N., Zhu, S., Zhang, D., Xu, S.: Synthesis and properties of magnetic Fe_3O_4-activated carbon nanocomposite particles for dye removal, *Mater. Lett.*, **62**, 645 – 647, (2008).

12 Zhang, B. B. *et al.*: Magnetic properties and adsorptive performance of manganese – zinc ferrites/activated carbon nanocomposites. *J. Solid State Chem.*, **221**, 302 – 305, (2015).

13 Fabris, D. *et al.*: Activated carbon/iron oxide magnetic composites for the adsorption of contaminants in water, *Carbon*, **40**, 2177 – 2183, (2002).

14 Ramanujan, R.V., Purushotham, S., Chia, M.H.: Processing and characterization of activated carbon coated magnetic particles for biomedical applications, *Mater. Sci. Eng. C*, **27**, 659 – 664, (2007).

15 Rybolt, T.R., Burrell, D.E., Shults, J.M., Kelley, A.K.: A biomedical application of activated carbon adsorption: an experiment using acetaminophen and n-acetylcysteine, *J. Chem. Educ.*, **65**, 1009, (1988).

16 Saha, D., Warren, K.E., Naskar, A.K.: Soft-templated mesoporous carbons as potential materials for oral drug delivery, *Carbon*, **71**, 47 – 57, (2014).

17 Hung, M.-C. *et al.*: Evaluation of active carbon fibers used in cell biocompatibility and rat cystitis treatment, *Carbon,* **68**, 628 – 637, (2014).

18 Chu, M. *et al.:* Laser light triggered-activated carbon nanosystem for cancer therapy, *Biomaterials*, **34**, 1820 – 1832, (2013).

19 Múzquiz-Ramos, E.M., Guerrero-Chávez, V., Macías Martínez, B.I., López-Badillo, C.M.: Synthesis and characterization of maghemite nanoparticles for hyperthermia applications, *Ceram. Int.*, **41**, 397 – 402, (2015).

20 Franckena, M. *et al.*: Hyperthermia dose-effect relationship in 420 patients with cervical cancer treated with combined radiotherapy and hyperthermia, *Eur. J. Cancer*, **45**, 1969 – 78, (2009).

21 Pradhan, P., Giri, J., Banerjee, R.: Preparation and characterization of manganese ferrite-based magnetic liposomes for hyperthermia treatment of cancer, *J. Magn. Magn. Mater.*, **311**, 208 – 215, (2007).

22 Boehm, H.P.: Some aspects of the surface chemistry, *Carbon*, **32**, 759 – 769, (1994).

23 Ríos-Hurtado, J.C., Múzquiz-Ramos, E.M., Zugasti-Cruz, A., Cortés-Hernández, D.A.: Mechanosynthesis as a simple method to obtain a magnetic composite (Activated Carbon/Fe_3O_4) for hyperthermia treatment, *J. Biomater. Nanobiotechnol.*, **7**, 19 – 28, (2016).

24 Caltun, O. *et al.*: The influence of mn doping level on magnetostriction coefficient of cobalt ferrite, *J. Magn. Magn. Mater.*, **316**, e618 – e620, (2007).

25 Atif, M., Sato Turtelli, R., Grössinger, R., Siddique, M., Nadeem, M.: Effect of mn substitution on the cation distribution and temperature dependence of magnetic anisotropy constant in $Co_{1-x}Mn_xFe_2O_4$ ($0.0 \leq x \leq 0.4$) ferrites, *Ceram. Int.*, **40**, 471 – 478, (2014).

26 Figuerola, A., Di Corato, R., Manna, L., Pellegrino, T.: From iron oxide nanoparticles towards advanced iron-based inorganic materials designed for biomedical applications, *Pharmacol. Res.*, **62**, 126 – 43, (2010).

27 Pankhurst, Q., Connolly, J.: Applications of magnetic nanoparticles in biomedicine, *J. Phys. D.*, **36**, 167 – 181, (2003).

28 *ASTMF-756, Standard practice for assessment of hemolytic properties of materials, Annual Book of ASTM Standards. Committee F04 Medical and Surgical Materials and Devices, Subcommittee F04.16 Biocompatibility Test Methods. Annual Book of ASTM Standards.* (2009).